



Variable Fluid Properties and Thermal Radiation Effects on Natural Convection Couette Flow through a Vertical Porous Channel

Abiodun O. Ajibade¹ and Yusuf A. Bichi^{1*}

¹Department of Mathematics, Ahmadu Bello University, Zaria, Nigeria.

Authors' contributions

This work was carried out in collaboration between both authors. Author AOA designed and guided the study while author YAB managed the literature searches, write up and analyzed the result of the study. Both authors read and approved the final manuscript.

Article Information

DOI: 10.9734/JAMCS/2019/v31i130100

Editor(s):

(1) Dr. Kai-Long Hsiao, Associate Professor, Taiwan Shoufu University, Taiwan.

Reviewers:

(1) Yahaya Shagaiya Daniel, Kaduna State University, Nigeria.

(2) Asad Ullah, Kohat University of Science & Technology, Pakistan.

Complete Peer review History: <http://www.sdiarticle3.com/review-history/47161>

Received: 07 December 2018

Accepted: 14 February 2019

Published: 14 March 2019

Original Research Article

Abstract

The present article investigates natural convection Couette flow through a vertical porous channel due to combined effects of thermal radiation and variable fluid properties. The fluid considered in the model is of an optically dense with all its physical properties assumed constant except for its viscosity and thermal conductivity which are temperature dependent. The flow equations are simplified using non-linear Rosseland heat diffusion and as a consequence it resulted to high non-linearity of the flow equations. Adomian decomposition method (ADM) is used to solve the emanating equations and the influences of the essential controlling physical parameters involved are presented on graphs, tables and were discussed. In the course of investigation; it was found that both the fluid velocity and its temperature within the channel were seen to increase with growing thermal radiation parameter while the fluid's velocity and temperature were observed to descend with increase in thermal conduction of the fluid. Similarly; the fluid velocity was found to increase with decrease in the fluid viscosity. To validate the accuracy of the present investigation; the results obtained here in have been compared with a published work where good agreement was found.

*Corresponding author: E-mail: ayusuf@fudutsinma.edu.ng;

Keywords: Couette flow; variable viscosity; variable thermal conductivity; thermal radiation; porous channel; ADM.

Nomenclature and Greek Symbols

Symbols	Interpretation	Unit
y'	Dimensional length	m
y	Dimensionless length	
g	Gravitational acceleration	ms^{-2}
k	Thermal conductivity	W/mK
T	Dimensional temperature	K
h	Dimensional channel width	m
T_w	Wall temperature	K
T_0	Ambient temperature	K
u, v	Dimensional velocity	ms^{-1}
ν	Kinematic viscosity	m^2s^{-1}
α	Thermal diffusivity	m^2s^{-1}
δ	Absorption coefficient	
β	Volumetric expansion coefficient	K^{-1}
μ	Dynamic Viscosity	$kgm^{-1}s^{-1}$
μ_0	Ambient fluid viscosity	$kgm^{-1}s^{-1}$
ε	Thermal conductivity variation parameter	
k_0	Ambient thermal conductivity	
q_r	Radiative heat flux	Wm^{-2}
c_p	Specific heat capacity at constant temperature	
ρ	Density of the fluid	kgm^{-3}
Gr	Grashop number	
H	Heat source/sink parameter	
ϕ	Temperature difference parameter	K
θ	Dimensionless temperature	
σ	Stefan-Boltzman constant	JK^{-1}
λ	Viscosity variation parameter	
\mathfrak{R}	Set of real numbers	
c	Suction parameter	
S	Heat generation/absorption parameter	
R	Buoyancy force distribution parameter	
Nu_0	Nusselt number on the heated plate	
Nu_1	Nusselt number on the cold plate	
τ_0	Skin friction on the heated plate	
τ_1	Skin friction on the cold plate	
M	Constant	

1 Introduction

Couette flow is a phenomenon in fluid flow which occurs due to the movement of bounding surface surrounding the fluid. In 1984, Yosutomi [1] reported that this method has been used in hydrodynamics

lubrication in fluid machinery involving moving parts as a fundamental method for measurement of viscosity and as a mean of estimating the drag force in many wall driven applications.

Studies of convective heat transfer flows through porous media has been conducted by many researchers in view of its application in sciences and engineering; particularly in the utilization of geothermal energy, high performance building insulation, crude oil extraction in petroleum industries, solid matrix exchangers, chemical catalytic reactor, underground disposal of nuclear waste materials and many others. In the flow of viscous fluid, when varying viscosity property included, the flow characteristics change substantially compared to the constant case (Gray [2]). The study of Macosco [3] stated that when a fluid is under working conditions, the fluid can be subjected to extreme conditions such as high temperature, pressure and shear rate and as a consequence its viscosity is affected. Kafousius and Rees [4] concluded that when viscosity of any working fluid is sensitive to temperature variation, the effect of temperature-dependent viscosity has to be considered otherwise considerable errors may results in the heat transfer characteristics. Other correlated studies can be seen in Iyer et al. [5], Ingham and Pop [6], Neild and Bejan [7], Urbano and Nasuti [8], Daniel [9] and Prenay et al. [10].

Boundary layer flows with temperature-dependent thermal conductivity has been studied by investigators owing to its numerous applications in engineering technology as in the extrusion of plastic sheets, polymer processing, spinning of fibers, cooling of elastic sheets etc. Cooling procedure has to be controlled effectively as the quality of final products in manufacturing industries relies on the rate of heat transfer. In heat sink/ source applications; materials of high thermal conductivity are widely used while those of low conductivity are used as insulators. For example, liquid metals having Prandtl number in the range 0.01 – 0.1 are generally used as coolants because of their high thermal conductivity. The studies of Van den Berg et al. [11] has shown that variable thermal conductivity can delay secular cooling of mantle with constant viscosity model while that of Sharma and Aisha [12] disclosed that thermal conduction increases with decrease in Prandtl number. Similar interrelated studies can be observed in Dubuffet [13], Hofmeister [14], Starlin et al. [15], van den Berg et al. [16], Rihab et al. [17] and Blas [18].

Entropy generation is a measure of destruction of the available work done by a system; when it occurs it resulted to the emission of heat in the form of electromagnetic rays termed as “thermal radiation”. Thermal radiation is of fundamental importance in system maintenance as in human body for temperature regulation, heat source or sink application in electric cookers, drying of agricultural products, warming of houses e.t.c. For minimization of radiation effects on free convection flows especially in working medium that requires liberation of heat to the surrounding environment. Rosseland [19] m gave an expression for radiative heat flux which was later simplified by Sparrow and Cess [20] and is being widely used in the study of heat transfer with thermal radiation by scholars In view of this innovation, some researchers have adopted it and can be viewed in Elbasbeshy and Bazid [21], Schlichting and Mahmud [22], Ibanez et al. [23], Makinde [24], Makinde et al. [25], Makinde and Ogulu [26] and Ibrahim and Makinde [27]. In some of the above mentioned studies, the authors discussed the effect of thermal radiation using linearized Rosseland heat diffusion and this was later faulted by Magyari and Pantokratoras [28] on the basis that it does not reflects the real mechanism in heat transfer characteristics in most boundary layer flows with thermal radiation and they therefore gave alternative approach using non-linear Rossland heat diffusion. In apprehension of this achievement, correlated studies can be observed in Yabo et al. [29], Jha et al. [30] and Ajibade and Bichi [31].

This paper investigates variable fluid properties on steady natural convection Couette flow through a vertical porous channel. In particular; the variable fluid properties considered are that, the viscosity and thermal conductivity assumed variable status following Carey and Mollendorf [32] with the radiative heat flux adopting non-linear Rossland heat diffusion.

2 Mathematical Formulation

The schematic diagram below in Fig. 1 consists of an infinite vertical channel formed by two parallel plate stationed h distance apart. The channel is filled with an optically dense viscous incompressible fluid at the

expense of radiative heat flux of intensity q_r ; which is absorbed by the plates and transferred to the fluid. The fluid's physical properties are assumed constant except for its viscosity and thermal conductivity which are temperature dependent. Since the fluid is an optically dense; the radiative heat flux of Rosseland heat diffusion can be utilized to analyze the energy equation in the flow formation. The x' -axis is taken along the channel in the vertically upward direction, being the direction of the flow while the y' -axis is taken normal to it and the effect of radiative heat flux in the x' - direction is considered negligible compared to that in the y' - direction. The temperature of the plate kept at $y' = 0$ rise to T_w and thereafter maintained constant while the other plate at $y' = h$ remain at T_0 . Also, the plate at $y' = 0$ moves at its own plate impulsively at uniform velocity $u' = Mu_0$ while the other plate remains at rest.

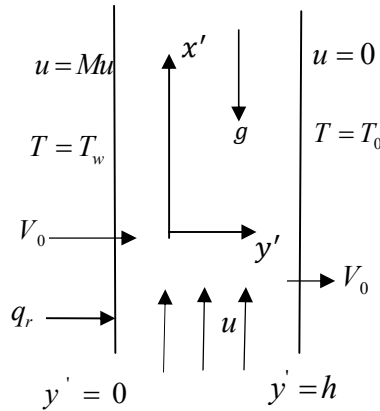


Fig. 1. Schematic diagram of the problem

The basic equations in vector form governing the flow of viscous incompressible fluid are:

Conservation of mass

$$\nabla \cdot \vec{\mathbf{v}} = 0 \tag{1}$$

Conservation of momentum

$$\frac{\partial \vec{\mathbf{v}}}{\partial t} + \left(\nabla \cdot \vec{\mathbf{v}} \right) \vec{\mathbf{v}} = -\frac{1}{\rho} \nabla p + \nu \nabla^2 \vec{\mathbf{v}} + \vec{\mathbf{g}} \tag{2}$$

Conservation of energy

$$\frac{\partial T}{\partial t} + \left(\vec{\mathbf{v}} \cdot \nabla \right) T = \frac{\kappa}{\rho c_p} \nabla^2 T + \frac{H}{\rho c_p} \tag{3}$$

where $\nabla = \frac{\partial}{\partial x} i + \frac{\partial}{\partial y} j + \frac{\partial}{\partial z} k$

The flow is considered two dimensional and fully developed so that $\vec{v} = (u, v, 0)$ with the flow direction assumed along the x' so that equation (1) reduces to:

$$\frac{dv}{dy} = 0 \quad (4)$$

Integrating equation (4) gives $v = V_0$ (a constant) which represents the velocity of suction /injection.

On utilizing Makinde *et al.*²⁵ (2007) and incorporating the effect of both variable fluid viscosity and thermal conductivity, the governing momentum and energy equations at steady sate are thus:

$$V_0 \frac{\partial u'}{\partial y'} + \frac{1}{\rho} \frac{\partial}{\partial y'} \left(\mu \frac{\partial u'}{\partial y'} \right) + g\beta(T - T_0) = 0 \quad (5)$$

$$V_0 \frac{\partial T'}{\partial y'} + \frac{1}{\rho c_p} \frac{\partial}{\partial y'} \left(k \frac{\partial T'}{\partial y'} \right) - \frac{1}{\rho c_p} \frac{\partial q_r}{\partial y'} = 0 \quad (6)$$

where the radiative heat flux (q_r) has the form:

$$q_r = \frac{-4\sigma \partial T'^4}{3\delta \partial y'} \quad (\text{Sparrow and Cess}^{20} (1978)) \quad (7)$$

Following Carey and Mollendorf³² (1978); the fluid viscosity (μ) and thermal conductivity (k) are respectively of the form:

$$\mu = \mu_0 \left(1 - \lambda \left(\frac{T - T_0}{T_w - T_0} \right) \right), k = k_0 \left(1 - \varepsilon \left(\frac{T - T_0}{T_w - T_0} \right) \right) \quad \text{for } \lambda, \varepsilon \in \Re \quad (8)$$

The following initial and boundary conditions for the velocity and temperature fields are employed:

$$u' = 0, T' = T_0 \quad \text{for } 0 \leq y' \leq h \quad (9)$$

$$\begin{cases} u' = Mu_0, T' = T_w & \text{at } y' = 0 \\ u' = 0, T' = T_0 & \text{at } y' = h \end{cases} \quad (10)$$

The meanings of all the physical quantities involved are given in the nomenclature.

The following dimensionless quantities as given by Ajibade et al. [33] are adopted:

$$u = \frac{u'}{u_0}, y = \frac{y'}{h}, \theta(y) = \frac{T' - T_0}{T_w - T_0} \quad (11)$$

Using equations (7), (8) and (11) in equation (5), the equation for the velocity field in dimensionless form is:

$$u''(y) = -c(1 + \lambda\theta(y))u'(y) + \lambda(1 + \lambda\theta(y))\theta'(y)u'(y) - Gr\theta(y)(1 + 2\lambda\theta(y)) \quad (12)$$

Following Magyari and Pantokratoras²⁸ (2011) and using equation (11); $\frac{\partial q_r}{\partial y'}$ is expanded as follow:

$$\begin{aligned} \frac{\partial q_r}{\partial y'} &= \frac{\partial}{\partial y'} \left[\left(-\frac{4\sigma}{3\delta} \right) \frac{\partial T''}{\partial y'} \right] = -\frac{4\sigma}{3h^2\delta} \left(\frac{\partial^2}{\partial y'^2} \left([\theta(y)(T_w - T_0) + T_0]^4 \right) \right) \\ &= -\frac{4\sigma}{3h^2\delta} \left(\frac{\partial}{\partial y'} \left(4[\theta(y)(T_w - T_0) + T_0]^3 \right) \frac{\partial}{\partial y'} (\theta(y)(T_w - T_0)) \right) \\ &= -\frac{4\sigma}{3h^2\delta} \left(12[\theta(y)(T_w - T_0) + T_0]^2 \frac{\partial}{\partial y'} (\theta(y)(T_w - T_0)) \frac{\partial}{\partial y'} (\theta(y)(T_w - T_0)) \right) \\ &\quad - \frac{4\sigma}{3h^2\delta} \left(4[\theta(y)(T_w - T_0) + T_0]^3 \frac{\partial^2}{\partial y'^2} (\theta(y)(T_w - T_0)) \right) \\ &= -\frac{4\sigma}{3h^2\delta} \left(12(T_w - T_0)^4 [\theta(y) + \phi]^2 \theta'(y)\theta'(y) \right) \\ &\quad - \frac{4\sigma}{3h^2\delta} \left(4(T_w - T_0)^4 [\theta(y) + \phi]^3 \theta''(y) \right) \end{aligned} \quad (13)$$

Substituting equation (8), (11) and (13) in equation (2) and rearranging, the following equation is achieved:

$$\begin{aligned} \theta''(y) &= -c\theta'(y)(1 + \varepsilon\theta(y)) \left[1 - \frac{4R_T}{3}(1 + \varepsilon\theta(y))[\theta(y) + \phi]^3 \right] \\ &\quad - 4R_T(1 + \varepsilon\theta(y))\theta'^2(y)[\theta(y) + \phi]^2 \left[1 - \frac{4R_T}{3}(1 + \varepsilon\theta(y))[\theta(y) + \phi]^3 \right] \end{aligned} \quad (14)$$

Again; on using equation (11) in equations (9– 10), the initial and boundary conditions are now:

$$u = 0, \theta = 0 \quad \text{for } 0 \leq y \leq 1 \quad (15)$$

$$\begin{cases} u = M, \theta = 1 & \text{at } y = 0 \\ u = 0, \theta = 0 & \text{at } y = 1 \end{cases} \quad (16)$$

Where $R_T = \frac{4\sigma(T_w - T_0)^3}{3k_0\delta}$, $\phi = \frac{T_0}{T_w - T_0}$, $c = \frac{hV_0}{\alpha}$ (17)

2.1 ADM Solution of the Problem

Adomian decomposition method popularly known as ADM was introduced by Adomian [34]. This method is based for the search of solutions of differential equations in the form of series in which the terms are calculated using recursive relations. Some of advantages over the known classical techniques include:

- i. It does not require discretization of the solution.
- ii. The method avoids perturbation in order to find conditions required for next computations
- iii. The method does not result in any large system of equations neither not is it affected by computational round off errors
- iv. It does not take long time and large amount of computer memory.
- v. It shows the interactions between the controlling parameters involved in a problem.

Equations (12) and (14) subject to the boundary conditions (15) and (16) are solved by ADM as follow:

Denote by $u''(y) = \frac{d^2u(y)}{dy^2}$ and let $L = \frac{d^2u(y)}{dy^2}$ so that

$$Lu(y) = u''(y) \text{ and } L\theta(y) = \theta''(y) \tag{18}$$

Using equation (18); equations (12) and (14) can be written as:

$$Lu(y) = -c(1 + \lambda\theta(y))u'(y) + \lambda(1 + \lambda\theta(y))\theta'(y)u'(y) - Gr\theta(y)(1 + 2\lambda\theta(y)) \tag{19}$$

$$L\theta(y) = -c\theta'(y)(1 + \varepsilon\theta(y)) \left[1 - \frac{4R_T}{3}(1 + \varepsilon\theta(y))[\theta(y) + \phi]^3 \right] + \varepsilon L^{-1} \left\{ \theta'^2(y)(1 + \varepsilon\theta(y)) \left[1 - \frac{4R_T}{3}(1 + \varepsilon\theta(y))[\theta(y) + \phi]^3 \right] \right\} - 4R_T L^{-1} \left\{ (1 + \varepsilon\theta(y))\theta'^2(y)[\theta(y) + \phi]^2 \left[1 - \frac{4R_T}{3}(1 + \varepsilon\theta(y))[\theta(y) + \phi]^3 \right] \right\} \tag{20}$$

Operating L^{-1} both sides of equations (19) and (20) we obtain:

$$L^{-1}Lu(y) = -cL^{-1} \left\{ (1 + \lambda\theta(y))u'(y) \right\} + \lambda L^{-1} \left\{ (1 + \lambda\theta(y))\theta'(y)u'(y) \right\} - GrL^{-1} \left\{ \theta(y)(1 + 2\lambda\theta(y)) \right\} \tag{21}$$

$$L^{-1}L\theta(y) = -cL^{-1} \left\{ \theta'(y)(1 + \varepsilon\theta(y)) \left[1 - \frac{4R_T}{3}(1 + \varepsilon\theta(y))[\theta(y) + \phi]^3 \right] \right\} + \varepsilon L^{-1} \left\{ \theta'^2(y)(1 + \varepsilon\theta(y)) \left[1 - \frac{4R_T}{3}(1 + \varepsilon\theta(y))[\theta(y) + \phi]^3 \right] \right\} - 4R_T L^{-1} \left\{ (1 + \varepsilon\theta(y))\theta'^2(y)[\theta(y) + \phi]^2 \left[1 - \frac{4R_T}{3}(1 + \varepsilon\theta(y))[\theta(y) + \phi]^3 \right] \right\} \tag{22}$$

Where $L^{-1} = \int \int (\bullet) dy dy$

By ADM:

$$L^{-1}Lu(y) = u(y) - u(0) - yu'(0) \tag{23}$$

$$L^{-1}L\theta(y) = \theta(y) - \theta(0) - y\theta'(0) \tag{24}$$

Using equation (9), (23) and (24) in equations (21) and (22) we have:

$$u(y) = M + yA - cL^{-1} \left\{ (1 + \lambda\theta(y))u'(y) \right\} + \lambda L^{-1} \left\{ (1 + \lambda\theta(y))\theta'(y)u'(y) \right\} - GrL^{-1} \left\{ \theta(y)(1 + 2\lambda\theta(y)) \right\} \tag{25}$$

$$\begin{aligned} \theta(y) = & 1 + yB - cL^{-1} \left\{ \theta'(y)(1 + \varepsilon\theta(y)) \left[1 - \frac{4R_T}{3}(1 + \varepsilon\theta(y))[\theta(y) + \phi]^3 \right] \right\} \\ & + \varepsilon L^{-1} \left\{ \theta'^2(y)(1 + \varepsilon\theta(y)) \left[1 - \frac{4R_T}{3}(1 + \varepsilon\theta(y))[\theta(y) + \phi]^3 \right] \right\} \\ & - 4R_T L^{-1} \left\{ (1 + \varepsilon\theta(y))\theta'^2(y)[\theta(y) + \phi]^2 \left[1 - \frac{4R_T}{3}(1 + \varepsilon\theta(y))[\theta(y) + \phi]^3 \right] \right\} \end{aligned} \tag{26}$$

Where $A = f'(0)$ and $B = \theta'(0)$ are assumed values to be determined based on the boundary condition in equation (10).

According to standard ADM, $u(y)$ and $\theta(y)$ can be expressed in the forms:

$$u(y) = \sum_{n=0}^{\infty} u_n(y) \quad \text{and} \quad \theta(y) = \sum_{n=0}^{\infty} \theta_n(y) \tag{27}$$

Using equation (27) in equations (25) and (26), we have:

$$\begin{aligned} \sum_{n=0}^{\infty} u_n(y) = & M + yA - cL^{-1} \left\{ \left(1 + \lambda \sum_{n=0}^{\infty} \theta_n(y) \right) \frac{d}{dy} \left(\sum_{n=0}^{\infty} u_n(y) \right) \right\} \\ & + \lambda L^{-1} \left\{ \left(1 + \lambda \sum_{n=0}^{\infty} \theta_n(y) \right) \frac{d}{dy} \sum_{n=0}^{\infty} (\theta_n(y)) \frac{d}{dy} \sum_{n=0}^{\infty} (u_n(y)) \right\} \\ & - GrL^{-1} \left\{ \sum_{n=0}^{\infty} \theta_n(y) \left(1 + 2\lambda \sum_{n=0}^{\infty} \theta_n(y) \right) \right\} \end{aligned} \tag{28}$$

$$\begin{aligned} \sum_{n=0}^{\infty} \theta_n(y) = & 1 + yB - cL^{-1} \left\{ \frac{d}{dy} \left(\sum_{n=0}^{\infty} \theta_n(y) \right) \left(1 + \varepsilon \sum_{n=0}^{\infty} \theta_n(y) \right) \left[1 - \frac{4R_T}{3} \left(1 + \varepsilon \sum_{n=0}^{\infty} \theta_n(y) \right) \left[\sum_{n=0}^{\infty} \theta_n(y) + \phi \right]^3 \right] \right\} \\ & + \varepsilon L^{-1} \left\{ \frac{d^2}{dy^2} \left(\sum_{n=0}^{\infty} \theta_n(y) \right) \left(1 + \varepsilon \sum_{n=0}^{\infty} \theta_n(y) \right) \left[1 - \frac{4R_T}{3} \left(1 + \varepsilon \sum_{n=0}^{\infty} \theta_n(y) \right) \left[\sum_{n=0}^{\infty} \theta_n(y) + \phi \right]^3 \right] \right\} \\ & - 4R_T L^{-1} \left\{ \left(1 + \varepsilon \sum_{n=0}^{\infty} \theta_n(y) \right) \left[\sum_{n=0}^{\infty} \theta_n(y) + \phi \right]^2 \frac{d^2}{dy^2} \left(\sum_{n=0}^{\infty} \theta_n(y) \right) \left[1 - \frac{4R_T}{3} \left(1 + \varepsilon \sum_{n=0}^{\infty} \theta_n(y) \right) \left[\sum_{n=0}^{\infty} \theta_n(y) + \phi \right]^3 \right] \right\} \end{aligned} \tag{29}$$

Setting $\theta_0(y) = 1 + By$ and $u_0(y) = M + yA - GrL^{-1} \{(1 + 2\lambda\theta(y))\theta(y)\}$ (30)

then $u_{n+1}(y)$ and $\theta_{n+1}(y)$ for $n \geq 0$ are determined using the recursive relations:

$$u_{n+1}(y) = -cL^{-1} \left\{ \left(1 + \lambda\theta_n(y) \frac{d}{dy} (u_n(y)) \right) \right\} + \lambda L^{-1} \left\{ (1 + \lambda\theta_n(y)) \frac{d}{dy} (\theta_n(y)) \frac{d}{dy} (u_n(y)) \right\} \quad (31)$$

$$\begin{aligned} \theta_{n+1}(y) = & -cL^{-1} \left\{ \frac{d}{dy} (\theta_n(y)) (1 + \varepsilon\theta_n(y)) \left[1 - \frac{4R_r}{3} (1 + \varepsilon\theta_n(y)) [\theta_n(y) + \phi] \right]^3 \right\} \\ & + \varepsilon L^{-1} \left\{ \frac{d}{dy} (\theta_n(y)) \frac{d}{dy} (\theta_n(y)) (1 + \varepsilon\theta_n(y)) \left[1 - \frac{4R_r}{3} (1 + \varepsilon\theta_n(y)) [\theta_n(y) + \phi]^3 \right] \right\} \\ & - 4R_r L^{-1} \left\{ (1 + \varepsilon\theta_n(y)) \frac{d^2}{dy^2} (\theta_n(y)) [\theta_n(y) + \phi]^2 \left[1 - \frac{4R_r}{3} (1 + \varepsilon\theta_n(y)) [\theta_n(y) + \phi]^3 \right] \right\} \end{aligned} \quad (32)$$

For details on ADM refer to Adomian³⁴ (1994).

2.2 Convergence of the ADM Solution and Termination Criterion of the Problem

Adomian [34] and Cherrault [35] have discussed intensively on the convergence of ADM. Nevertheless; to verify the convergence of the ADM solution in the present problem; the method of ratio test is deployed. Using computer algebra package the following terms were obtained at

$y = 0.5, M = 1, c = 0.1, \lambda = 0.1, Gr = 10, \phi = 0.1, R_r = 0.1, \varepsilon = 0.1$ as:

$\theta_0 = 0.5124042184, \theta_1 = -0.1703022291, \theta_2 = 0.0003468323623, \theta_3 = 4.31320421237 \times 10^{-6}$

$u_0 = 1.190089496, u_1 = -0.02996349680, u_2 = 0.001461778228, u_3 = -0.00004598585703$ (33)

and

$$\begin{aligned} \left| \frac{\theta_1}{\theta_0} \right| &= 0.03323591473, & \left| \frac{\theta_2}{\theta_1} \right| &= 0.02036569716, & \left| \frac{\theta_3}{\theta_2} \right| &= 0.01243599122 \\ \left| \frac{u_1}{u_0} \right| &= 0.02517751556, & \left| \frac{u_2}{u_1} \right| &= 0.04878530159, & \left| \frac{u_3}{u_2} \right| &= 0.03145884659 \end{aligned} \quad (34)$$

Numerical values in equation (30) shows that

$$\lim_{j \rightarrow \infty} \left| \frac{f_{j+1}}{f_j} \right| < 1, \text{ for } j \geq 0 \text{ Robert [36]} \quad (35)$$

Hence the ADM solution of the present problem converges. For a meaningful series solution, the series needs to be truncated at a point such that the contribution of any additional term is negligible to the final solution. As such a termination criterion is used such that the series is truncated whenever $|u_i, \theta_i| < \varepsilon$. For the present problem, we have chosen $\varepsilon = 3.5 \times 10^{-4}$. Considering this assumption, the solution for u and θ are thus truncated after the 3rd terms. Due to huge size of the computed ADM solution, the solutions are not displayed here rather they are used for numerical computations for the purpose of discussing the result.

2.3 Nusselt number and Skin Friction

Following Kay [37], the Nusselt number on the channel plates stationed at $y = 0$ and $y = 1$ are respectively evaluated using:

$$Nu_0 = (1 - \varepsilon\theta(y)) \frac{d\theta}{dy} \Big|_{y=0} \quad \text{and} \quad Nu_1 = (1 - \varepsilon\theta(y)) \frac{d\theta}{dy} \Big|_{y=1} \quad (36)$$

while the skin frictions on the channel plates are calculated via:

$$\tau_0 = (1 - \lambda\theta(y)) \frac{du(y)}{dy} \Big|_{y=0} \quad \text{and} \quad \tau_1 = (1 - \lambda\theta(y)) \frac{du(y)}{dy} \Big|_{y=1} \quad (37)$$

3 Results and Discussion

The present article investigated variable fluid properties and thermal radiation effects on natural convection Couette flow through a vertical porous channel using nonlinear Rosseland heat diffusion. Computer simulation was conducted on the solution of the flow equations considering the influence of the essential physical parameters involved and the results are presented in figure 2 – 11 and on tables I - III. For the purpose of discussion of this result, the value of R_T and ε are taken within the range $0 \leq R_T, \varepsilon \leq 1$ for which the solution of the governing equations are convergent. Similarly, the values for ϕ , λ and M has been chosen arbitrarily between 0.1 – 3 while that of Gr are selected as 10, 12 and 14.

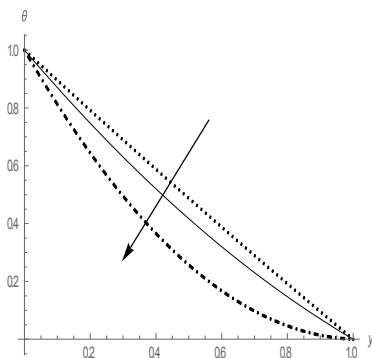


Fig. 2. Temperature profiles for different values of c
 $(\phi = 0.1, R_T = 0.1, \lambda = 0.1, \varepsilon = 0.1, c = \{0.1, 0.5, 1\})$

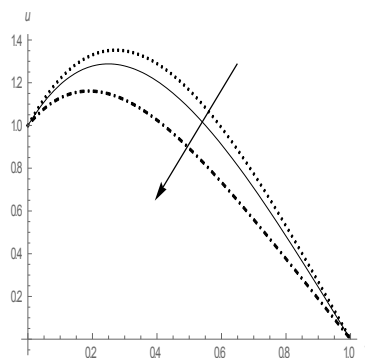


Fig. 3. Velocity profiles for different values of c
 $(\phi = 0.1, R_T = 0.1, Gr = 10, \lambda = 0.1, M = 0.1, \varepsilon = 0.1, c = \{0.1, 0.5, 1\})$

Figs. 2 and 3 displayed the effects of suction parameter (c) on the velocity and temperature of the fluid within the channel where the figures show that both the temperature and velocity decreases with growing c . These behaviors are accredited to the decrease in thermal diffusivity of the working fluid with growing c .

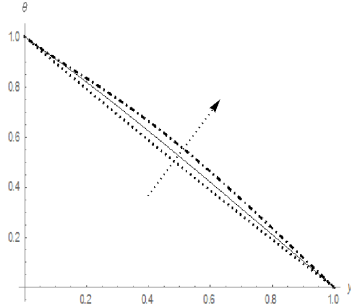


Fig. 4. Temperature profiles for different values of R_T
 ($\phi = 0.1, c = 0.1, \epsilon = 0.1, \dots R_T = 0.01, \dots R_T = 0.4, \dots R_T = 0.8$)

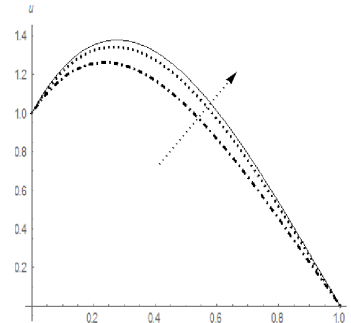


Fig. 5. Velocity profiles for different values of R_T
 ($\phi = 0.1, c = 0.1, \lambda = 0.1, Gr = 10, M = 1, \phi = 0.1, \epsilon = 0.1, \dots R_T = 0.001, \dots R_T = 0.4, \dots R_T = 0.8$)

The effect of thermal radiation parameter (R_T) on the fluid temperature is naked in Fig. 4 where the figure shows that the temperature within the channel increases with increase in R_T . The resulting effect of this has transferred to increase the velocity of the fluid within the channel as graphed in Fig. 5. These attitudes are inclined to the decrease in thermal conduction of the fluid in the channel.

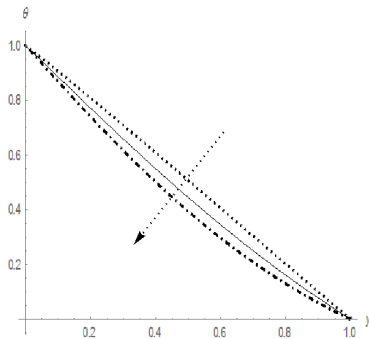


Fig. 6. Temperature profiles for different values of ϵ
 ($\phi = 0.1, c = 0.1, R_T = 0.01, \dots \epsilon = 0.1, \dots \epsilon = 0.4, \dots \epsilon = 0.5$)

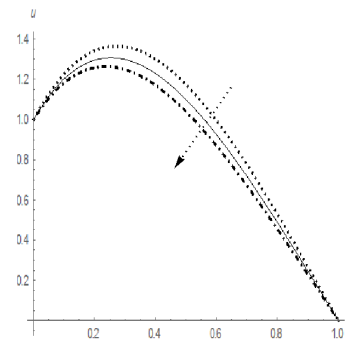


Fig. 7. Velocity profiles for different values of ϵ
 ($\phi = 0.1, c = 0.1, \lambda = 0.1, M = 1, R_T = 0.01, \dots \epsilon = 0.1, \dots \epsilon = 0.4, \dots \epsilon = 0.5$)

Figs. 6 and 7 presents the effect of thermal conduction parameter (ϵ) on the velocity and temperature of the fluid within the channel where it is eyed from the figures that, an increase in ϵ contributes to the decrease in the temperature and velocity of the fluid within the channel. This is attributed to the decrease in thermal conduction of the fluid which act to diminish the influence of the applied boundary temperature and thus causing a decrease in the thermodynamics and hydrodynamics of fluid within the channel.

Fig. 8 depicts the influence of viscosity variation parameter (λ) on the fluid velocity in the channel where it is seen that the velocity of the fluid escalate with increase in λ . This is credited to the decrease in the fluid's viscosity within the channel.

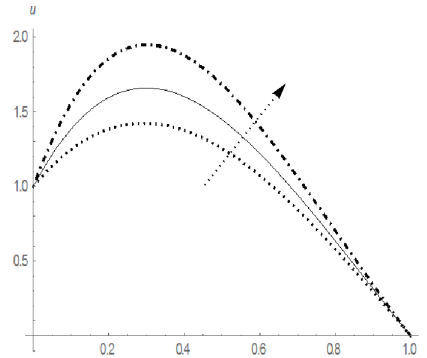


Fig 8. Velocity profile for different values of λ

($\phi = 0.1, c = 0.1, M = 1, Gr = 10, \epsilon = 0.1, R_T = 0.1, \dots \lambda = 0.1, \text{---} \lambda = 0.4, \text{---} \lambda = 0.7$)

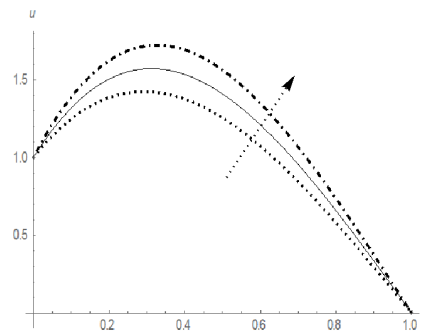


Fig 9. Velocity profile for different values of Gr

($\phi = 0.1, c = 0.1, M = 1, \lambda = 0.1, \epsilon = 0.1, R_T = 0.1, \dots Gr = 10, \text{---} Gr = 12, \text{---} Gr = 12$)

The effect of varying Gr is pictured in figure 9 where the figure shows that the fluid velocity within the channel increases with ascending Gr. This is accredited to the increase in the buoyancy force of the fluid molecules within the channel and hence an increase in the fluid velocity.

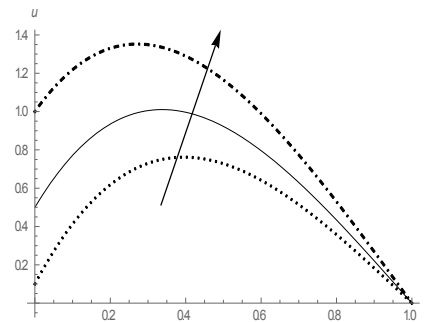


Fig 10. Velocity profile for different values of M

($\phi = 0.1, c = 0.1, \lambda = 0.1, Gr = 10, \epsilon = 0.1, R_0 = 0.1, \dots M = 0.1, \text{---} M = 0.5, \text{---} M = 1$)

Fig. 10 reflects the effect of varying the velocity of the moving boundary on the fluid velocity within the channel. The figure demonstrated that the velocity of the fluid increases with increase M. This is practically

true that in no-slip regime, the thin film of the fluid adjacent to the moving plate moves with the velocity of the moving plate.

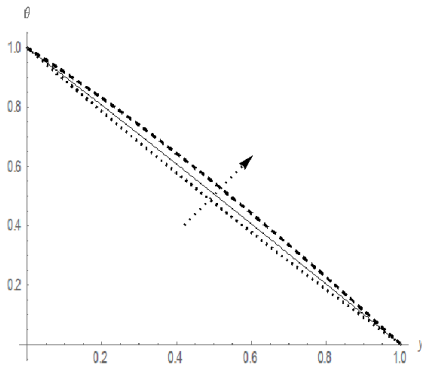


Fig. 11. Temperature profile for different values of ϕ
 ($M = 1, c = 0.1, \lambda = 0.1, Gr = 10, \epsilon = 0.1, R_T = 0.1,$
 $\phi = 2$, _____ $\phi = 4$, -.-.- $\phi = 6$)

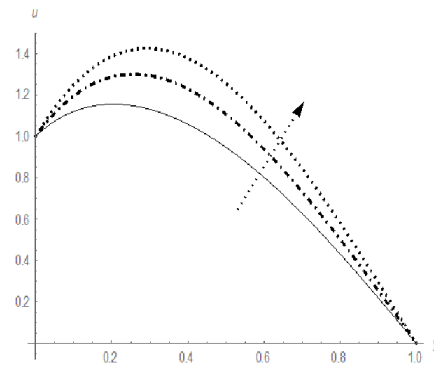


Fig. 12. Velocity profile for different values of ϕ
 ($M = 1, c = 0.1, \lambda = 0.1, Gr = 10, \epsilon = 0.1, R_T = 0.1,$
 _____ $\phi = 2$, .-.-. $\phi = 4$, $\phi = 6$)

The effect of temperature difference parameter (ϕ) is shown in Figs. 11 and 12. These figures displayed that the velocity and temperature of the fluid within the channel increases with increase in ϕ . This is owing to the decrease in ambient temperature of the fluid in the channel.

Table 1. Nusselt number on the channel plates

R_T	$\epsilon = 0.01, \phi = 0.1,$ $c = 0.1$		$\epsilon = 0.04, \phi = 0.1,$ $c = 0.1$		$\epsilon = 0.04, \phi = 0.4,$ $c = 0.1$		$\epsilon = 0.04, \phi = 0.4,$ $c = 0.4$	
	Nu_0	Nu_1	Nu_0	Nu_1	Nu_0	Nu_1	Nu_0	Nu_1
0.01	1.03354	0.94317	1.02032	0.92850	1.00723	0.93737	1.1999	0.73108
0.04	1.00392	0.96424	0.97840	0.94748	0.93906	0.97863	1.08756	0.79980
0.06	0.970875	0.97511	0.95426	0.95945	0.90514	1.00234	1.03279	0.83811
0.08	0.95023	0.98557	0.93271	0.97090	0.87807	1.02349	0.98932	0.87162
0.1	0.93166	0.99563	0.91341	0.98184	0.85651	1.04243	0.95456	0.90107

The effects of varying physical parameters on Nusselt numbers is presented on Table 1. The table displayed that for some fixed values of ϵ , ϕ and c ; Nu_0 decreases with increase in R_T while Nu_1 increases with increase in R_T . For small increase in ϵ ; both Nu_0 and Nu_1 decreases with growth in R_T . Furthermore; with slight increase in ϕ , Nu_0 decreases while Nu_1 increases. Again, with increase in c , Nu_0 increases while Nu_1 decreases.

Table 2 reflects the effect of varying parameters on the skin frictions between the working fluid and the channel plates. It is viewed from the table that for some fixed values of parameters; the skin friction on the plates increases with increase in λ . Furthermore; with small increase in ϵ , c and R_T ; the skin friction on all the plates increases with increase in λ .

Table 2. Numerical values for skin friction on the channel plates

λ	$\varepsilon = 0.01, R_T = 0.01,$ $\phi = 0.1, c = 0.1,$ $Gr = 10, M = 1$		$\varepsilon = 0.04, R_T = 0.01,$ $\phi = 0.1, c = 0.1,$ $Gr = 10, M = 1$		$\varepsilon = 0.04, R_T = 0.04,$ $\phi = 0.1, c = 0.1,$ $Gr = 10, M = 1$		$\varepsilon = 0.04, R_T = 0.04,$ $\phi = 0.1, c = 0.3,$ $Gr = 10, M = 1$	
	τ_0	τ_1	τ_0	τ_1	τ_0	τ_1	τ_0	τ_1
0.1	2.83322	2.63734	2.81556	2.62253	2.84510	2.66538	2.93564	2.44038
0.3	3.91679	2.73376	3.89354	2.71849	3.90334	2.75920	4.08705	2.53810
0.5	5.19877	2.86072	5.17240	2.84718	5.19630	2.87401	5.46283	2.76598
0.7	7.02756	3.27627	7.00799	3.27001	7.03197	3.26943	8.13084	3.80993
0.9	11.3904	5.53925	11.4668	5.59259	11.7015	5.65006	33.0152	22.7099

4 Validation of the Result

To authenticate the validity of the result; the present result on setting $\lambda = \varepsilon = c = R_T = 0, M = 1$ is compared with that of the published work of Jha and Ajibade[38] on relaxing heat absorbing/ generating parameter and the comparison is tabulated below:

Table 3. Comparison between the results of Jha and Ajibade (2010) and the present study

y	Jha and Ajibade [38] when $S = 0$		Present study when $R_T = \varepsilon = 0$ and $M = 1$	
	$\theta(y)$	$u(y)$	$\theta(y)$	$u(y)$
0.1	0.9000	1.1850	0.9000	1.1850
0.3	0.7000	1.3000	0.7000	1.3000
0.5	0.5000	1.1250	0.5000	1.1250
0.7	0.3000	0.7600	0.3000	0.7600
0.9	0.1000	0.2650	0.1000	0.2650

Numerical values in Table 3 show that the two studies have good agreement between them.

5 Conclusion

Natural convection Couette flow through a vertical porous channel with thermal radiation and variable fluid properties effects was investigated using non-linear Rosseland heat diffusion, Adomian decomposition method and computer algebra package where results were presented and discussed. The major findings of the investigation are:

- i. The velocity and temperature of the fluid within the channel were found to decrease with increase in suction parameter.
- ii. Both the fluid velocity and temperature in the channel were discovered to descend with increase in thermal conduction parameter.
- iii. A decrease in the fluid viscosity was realized to ascend the fluid velocity within the channel.

Increase in thermal radiation parameter was recognized to rise both the fluid's temperature and velocity within the channel.

Competing Interests

Authors have declared that no competing interests exist.

References

- [1] Yasutomi S, Bair S, Winer WO. An application of a free volume model to lubricant rheology I. Dependence on viscosity on temperature and pressure. *J. Tribol. Trans. ASME*. 1984;106:291-303.
- [2] Gray J, Kassory DR, Tadjeran H, Zebib A. Effect of significant viscosity variation on convective heat transport in water-saturated porous media. *J. Fluid Mech.* 1982;117:233-249.
- [3] Macosco CW. *Rheology, principles, measurements and applications*. VCH Publishers, Inc. 1994;1-10.
- [4] Kafoussius NG, Rees DAS. Numerical study of the combined free and forced convective laminar boundary layer flow past a vertical isothermal flat plate with temperature-dependent viscosity. *Acta Mech.* 1998;127:39-50.
- [5] Iyer RS, Kak S, Fung KY. Instability and heat transfer in grooved channel flow. *J. Thermophysics and Heat Transfer*. 1997;11(3):437-445.
- [6] Ingham DB, Pop I. *Transport phenomena in porous media*. Pergamon. Oxford; 1998.
- [7] Neild DA, Bejan A. *Convection in porous media*. 4th Edition. Springer, New York; 2013.
- [8] Urbano A, Nasuti F. Onset of heat transfer deterioration in superficial methane flow channel. *J. Thermophysics Heat Trans.* 2013;27(2):278-308.
- [9] Daniel YS. MHD laminar flows and heat transfer adjacent to permeable stretching sheets with partial slip condition. *Journal of Advanced Mechanical Engineering*. 2017;4(1):1-15.
- [10] Prenay B, Suneet S, Hitesh B. A closed solution of dual lag heat conduction problem with time periodic boundary conditions. *J. Heat Trans.* 2019;141:031302.
- [11] Van den Berg AP, Rainey ESG, Yuen DA. The combined influence of variable thermal conductivity, temperature- and pressure- dependent viscosity and core-mantle coupling on thermal evolution. *Physics on the earth and planetary interiors*. 149:259-278, 2005.
- [12] Sharma, V. K. and Aisha, R. Effect of variable thermal conductivity and heat source/sink near a stagnation point on a linearly stretching sheet using HPM. *Global Journal of Sci. Frontier Research: Mathematics and Decision Making*. 2014;14(2):56-63.
- [13] Dubuffet F, Yuen DA, Rabinowicz M. Effects of a realistic mantle thermal conductivity on the patterns of 3D convection. *Earth Planet Sci. Lett.* 1999;171(3):401–409.
- [14] Hofmeister AM. Mantle values of thermal conductivity and the geotherm from phonon lifetimes. *Science*. 1999;283:1699–1706.
- [15] Starlin I, Yuen DA, Bergeron SY. Thermal evolution of sedimentary basin formation with temperature-dependent conductivity. *Geophys, Res, Lett.* 2000;27(02):265– 268.
- [16] Van den Berg AP, Yuen DA, Steinbach V. The effects of variable thermal conductivity on mantle heat-transfer. *Geophysical Research Letters*. 2001;285:875-878.
- [17] Rihab H, Raoudha C, Faouzi A, Abdelmajid J, Sassi BN. Lattice Boltzmann method for heat transfer with variable thermal conductivity. *Int, J. Heat and Technology*. 2017;35(2):313-324.

- [18] Blas Z. Effects of thermophysical variable properties on liquid sodium convective flows in a square enclosure. *J. Heat Trans.* 2019;141:031301.
- [19] Rosseland SE. *Astrophysik and atom-theoretische Grundlagen*. Springer-Verlag. Berlin. 1931;41-44.
- [20] Sparrow EM, Cess RD. *Radiation heat transfer*. Hemisphere Publishing Corporation. Washington; 1978.
- [21] Elbashbeshy EMA, Bazid MA. The effect of temperature dependent viscosity on heat transfer over a continuous moving surface. *J. App. Phy.* 2000;33:2716-2721.
- [22] Schlichting H, Mahmud S. Entropy generation in a vertical concentric channel with temperature dependent viscosity. *Int. Comm. Heat Mass Transfer.* 2002;29(7):907-918.
- [23] Ibanez G, Cuevas S, Lopez de Haro M. Minimization of entropy generation by asymmetric convective cooling. *International Journal in Heat and Mass Trans.* 2003;46:1321-1328.
- [24] Makinde OD. Free convection flow with thermal radiation and mass transfer past a moving vertical porous plate. *Int. Comm. Heat Mass Trans.* 2005;32:1411-1419.
- [25] Makinde OD, Olajuwon BI, Gbolagade AW. Adomian decomposition approach to a boundary layer flow with thermal radiation past a moving vertical porous plate. *Int. J. Applied Mathematics and Mech.* 2007;3(3):62-70.
- [26] Makinde OD, Ogulu A. The effect of thermal radiation on the heat and mass transfer flow of a variable viscosity fluid past a vertical porous plate permeated by a transversed magnetic field. *Chem. Eng. Comm.* 2008;195(12):1575-1584.
- [27] Makinde OD, Ibrahim SY. Radiation effect on chemically reacting magneto- hydrodynamics (MHD) boundary layer flow of heat and mass transfer through a porous vertical flat plate. *Int. J. Physical Sciences.* 2011;6(6):1508-1516.
- [28] Magyari E, Pantokratoras A. Note on the effect of thermal radiation in the linearised Rosseland approximation on the heat transfer characteristics of various boundary layer flows. *Int. Comm. Heat and Mass Tran.* 2011;38:554-556.
- [29] Yabo IB, Jha BK, Lin J. Combined effects of thermal diffusion and diffusion-thermo effects on transient MHD natural convection and mass transfer flow in a vertical channel with thermal radiation. *J. Applied Mathematics.* 2016;6:2354-2373.
- [30] Jha BK, Yabo IB, Lin J. Transient natural convection in an annulus with thermal radiation. *J. Applied Mathematics.* 2017;8:1351-1366.
- [31] Ajibade AO, Bichi YA. Unsteady natural convection flow through a vertical channel: Due to the combined effects of variable viscosity and thermal radiation. *J. Appl. Computat Math.* 2018;7(3):1-8.
- [32] Carey VP, Mollendorf JC. Natural convection in liquid with temperature dependent viscosity. In *Proceedings of the 6th International Heat Transfer Conference, Toronto.* 1998;2:211-217.
- [33] Ajibade AO, Jha BK, Omame A. Entropy generation under the effect of suction/injection. *J. Appl. Math. Modeling.* 2011;35:4630-4646.
- [34] Adomian G. *Solving frontier problems of physics: The decomposition method*. Boston, MA Kluwer; 1994.

- [35] Cherruault Y. Convergence of Adomian's method. J. Mathl Comput. Modelling. 1990;14:83-86.
- [36] Robert W, Murray RS. Schaum's outlines series for advanced calculus. Third Edition; 2010.
- [37] Kay A. Comments on 'combined effect of variable viscosity and thermal conductivity on free convection flow in a vertical channel using DTM' by J.C. Imavathi and M. Shekar. Meccanica. 2017;52(6):1493-1494.
- [38] Jha BK, Ajibade AO. Unsteady free convective couette flow of heat generating /absorbing fluid. Int. J. Energy Technology. 2010;2(12):1-9.

© 2019 Ajibade and Bichi; This is an Open Access article distributed under the terms of the Creative Commons Attribution License (<http://creativecommons.org/licenses/by/4.0>), which permits unrestricted use, distribution, and reproduction in any medium, provided the original work is properly cited.

Peer-review history:

The peer review history for this paper can be accessed here (Please copy paste the total link in your browser address bar)

<http://www.sdiarticle3.com/review-history/47161>